

Chemical Science

Accepted Manuscript



This is an *Accepted Manuscript*, which has been through the Royal Society of Chemistry peer review process and has been accepted for publication.

Accepted Manuscripts are published online shortly after acceptance, before technical editing, formatting and proof reading. Using this free service, authors can make their results available to the community, in citable form, before we publish the edited article. We will replace this *Accepted Manuscript* with the edited and formatted *Advance Article* as soon as it is available.

You can find more information about *Accepted Manuscripts* in the [Information for Authors](#).

Please note that technical editing may introduce minor changes to the text and/or graphics, which may alter content. The journal's standard [Terms & Conditions](#) and the [Ethical guidelines](#) still apply. In no event shall the Royal Society of Chemistry be held responsible for any errors or omissions in this *Accepted Manuscript* or any consequences arising from the use of any information it contains.

ARTICLE

Dehydrogenation of Formic Acid by Ir-bisMETAMORPhos Complexes: Experimental and Computational Insight in the Role of a Cooperative Ligand

Sander Oldenhof,^a Martin Lutz,^b Bas de Bruin,^a Jarl Ivar van der Vlugt,^a Joost N. H. Reek^{*a}

Cite this: DOI: 10.1039/x0xx00000x

Received 00th January 2012,
Accepted 00th January 2012

DOI: 10.1039/x0xx00000x

www.rsc.org/

The synthesis and tautomeric nature of three Xanthene-based bisMETAMORPhos ligands (**La-Lc**) is reported. Coordination of these bis(sulfonamide-phosphinamides) to Ir(acac)(cod) initially led to the formation of Ir^I(L^H) species (**1a**), which convert via formal oxidative addition of the ligand to Ir^{III}(L) monohydride complexes **2a-c**. The rates for this step strongly depend on the ligand employed. Ir^{III} complexes **2a-c** were applied in the base-free dehydrogenation of formic acid, reaching TOFs of 3090, 877 and 1791 h⁻¹, respectively. The dual role of the ligand in the mechanism of the dehydrogenation reaction was studied by ¹H and ³¹P NMR spectroscopy and DFT calculations. Besides functioning as an internal base, bisMETAMORPhos also assists in the pre-assembly of formic acid within the Ir-coordination sphere and aids in stabilizing the rate determining transition state through hydrogen-bonding.

Introduction

Enzyme active sites are a major source of inspiration for chemists in the field of synthetic chemistry and homogeneous catalysis, because of their high activities and selectivities achieved in chemical transformations and the conceptual strategies employed by these systems.¹ For instance, weak but highly directional hydrogen bonding stands out as key element used by enzymes to selectively pre-assemble and pre-activate substrates and stabilize transition states. Inspired by this, functional ligands decorated with H-bond donor and/or acceptor groups have been used to construct supramolecular ligand structures, enabling modular ligand families² to be utilized in transition metal catalysis and also for substrate pre-organization and pre-activation via specific ligand-substrate interactions.³

In our quest for novel systems able to undergo hydrogen-bonding interactions to steer reactivity we have developed sulfonamidophosphine (METAMORPhos) ligands. These ligands are based on a PNSO₂ scaffold that display NH-P / N=PH tautomerism (see Figure 1). They have been employed for mono- and bimetallic Rh-catalyzed hydrogenation, Ru-based heterolytic H₂ cleavage and [2+2+2] cycloaddition reactions.⁴

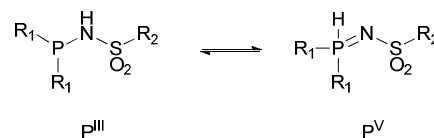


Fig 1. General composition of METAMORPhos ligands with their two tautomeric forms [NH-P (P^{III}) and N=PH (P^V)] in equilibrium.

Formate dehydrogenase metalloenzymes have successfully been employed for the reduction of CO₂ and oxidation of formate. Although there is no complete consensus concerning the mechanism of either the reduction or the oxidation, hydrogen-bonding and proton-shuttling are suggested to play a crucial role in the way these enzymes operate.⁵ We recently described our initial results with an Ir-catalyst bearing a bisMETAMORPhos ligand in the base-free catalytic dehydrogenation of formic acid. A reaction which has attracted much recent interest in the context of hydrogen storage/release systems.^{4f} Typically, formic acid (HCOOH) dehydrogenation catalysts require the addition of sub-stoichiometric amounts of base (e.g. 5:2 ratio of HCOOH:NEt₃) to facilitate substrate activation. However, this significantly reduces the overall

hydrogen weight percentage of the reaction mixture.⁶ One promising strategy to circumvent the use of exogenous base is to employ catalyst systems bearing cooperative ligands to access metal-ligand bifunctional pathways for substrate activation.⁷ Hydrogen-bonding interactions between ligand and substrate as (additional) tool to enhance reactivity have previously been proposed both in the hydrogenation of CO₂ and in the aluminium catalysed dehydrogenation of HCOOH.⁸ These interactions were also suggested to play a role in the formation of half-sandwich ruthenium and rhodium hydrides from formic acid.⁹ Several studies on the mechanism of HCOOH dehydrogenation have compared conventional β -hydride elimination with direct hydride-transfer (Figure 2A and B).¹⁰ Given the potential H-bonding abilities of METAMORPhos ligands and the protic nature of formic acid, we wondered if biomimetic non-covalent interactions between the ligand backbone and formic acid could play a role in this catalytic system. Herein we show that the proton-responsive ligand not only acts as internal base (Figure 2C), but that its hydrogen-bonding abilities steer substrate pre-assembly and stabilize catalytic transition states.

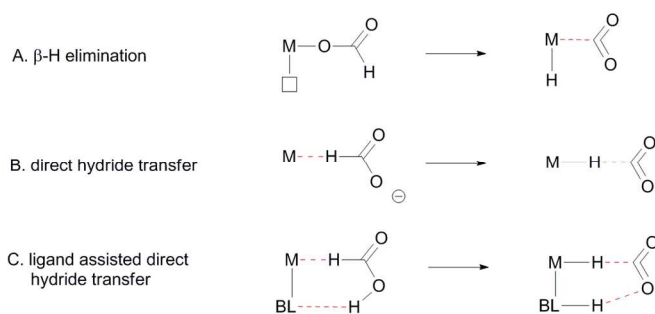


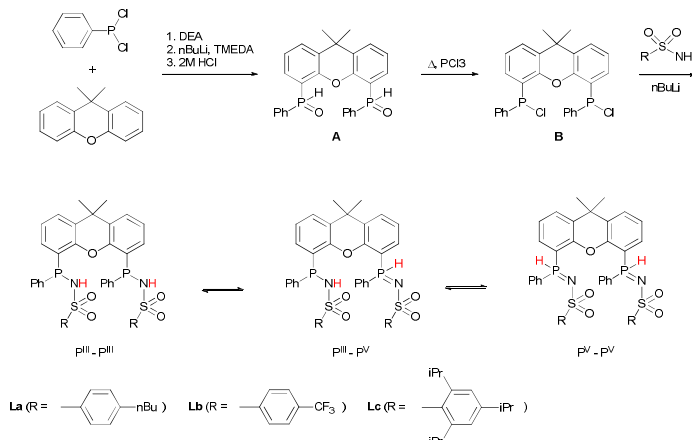
Fig 2. Different proposed mechanisms for the dehydrogenation of formic acid, BL: bifunctional ligand.

We will present the synthesis of three bisMETAMORPhos ligands as well as their coordination to iridium, compare the activity of these systems in HCOOH dehydrogenation and explain the dual role of the ligand framework during catalysis by means of both experimental and computational results.

Results and discussion

Synthesis of ligands and complexes

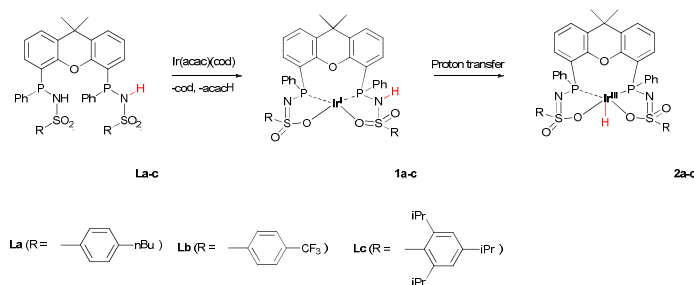
METAMORPhos ligands are prepared from a simple condensation reaction between a sulfonamide of choice and a chlorophosphine. They show high stability to both oxidation (at phosphorus) and hydrolysis (of the P-N bond). We attribute this stability to their prototropic character, resulting in an equilibrium between the P^{III} and P^V oxidation states that is influenced by R₁ and R₂.^{4c} In order to gain insight into the effect of ligand modification on the coordination and degree of tuning in HCOOH dehydrogenation catalysis, we prepared bisMETAMORPhos ligands **La-Lc** via a three-step synthetic protocol (Scheme 1) that results in selective formation of only the respective *meso*-isomers.[‡]



Scheme 1. The synthesis of bisMETAMORPhos ligands **La-Lc** and their three tautomeric forms (P^{III}-P^{III}, P^{III}-P^V and P^V-P^V).

All three ligands **La-Lc** display P^{III}/P^V tautomerism but in different ratios for the three possible forms. For ligand **La** only the P^{III}-P^{III} and P^{III}-P^V tautomers were observed in CD₂Cl₂ in a ratio of 1 : 0.4, as determined by ³¹P NMR spectroscopy. For both ligands **Lb** and **Lc** all three possible tautomers were observed, with ratios (P^{III}-P^{III}: P^{III}-P^V: P^V-P^V) of 1 : 1.8 : 0.2 and 1 : 1.9 : 0.1 for **Lb** and **Lc**, respectively. These data show that the overall P^{III}/P^V ratio is not only determined by the acidity of the N-H bond and basicity of the phosphorus atom but is also greatly influenced by steric bulk of the substituent on the sulfon group. The P^V tautomer provides stability in these ligands towards oxidation and hydrolysis, even to the extent that **La-Lc** can be conveniently purified by column chromatography. Upon coordination to a metal the tautomeric behaviour of these ligands is lost.

The addition of **La-Lc** to Ir^I(acac)(cod) generated complexes [Ir^I(L^H)] **1a-c** via a single proton-transfer from the ligand to acetylacetonate and displacement of cyclooctadiene. These species show highly fluxional behaviour between the protonated and deprotonated ligand arms, irrespective of the specific ligand substitution pattern, which therefore leads to symmetric ¹H and ³¹P NMR spectra. Formal oxidative addition of the remaining ligand -NH group in **1a-1c** generates the corresponding Ir^{III}(H)(L) complexes **2a-c** (Scheme 2).[‡]



Scheme 2. Synthesis of complex **1a-c** and **2a-c** from Ir^I(acac)(cod) and **La-c**.

The rates for this overall proton-transfer step vary significantly for ligands **1a-c**. Ir^{III} complex **2a** (with **La**) was obtained quantitatively after 30 hours at room temperature, but no

formation of complex **2b** was observed under the same conditions. This species could only be obtained after heating the mixture for 40 hours at 70 °C. In contrast, the conversion of **1c** into **2c** was significantly faster than the conversion of **1a** into **2a**, and full conversion was observed after already 16 hours at room temperature. We previously reported the molecular structure of **2a** to be dimeric in the solid state (**2a₂**), with the ‘vacant’ axial site coordinated by an oxygen from the sulfonamide of a second equivalent of **2a** (Figure 3a).^{4f} The molecular structure determined for the more bulky analogue **2c** was found to be a slightly distorted octahedral mononuclear Ir^{III} hydride complex, with axial coordination of a water molecule *trans* to the hydride to complete the octahedral coordination environment of Ir^{III} (see Figure 3b). The steric hindrance of the isopropyl groups in complex **2c** seems to effectively prevent the formation of dinuclear complexes as was also found by modelling studies. This finding also supports the previously proposed mononuclear configuration in solution, based on diffusion NMR data.^{4f} The N-S bond lengths of 1.554(2) Å are in agreement with deprotonated sulfonamide fragments.^[4f] The Ir-O_{water} bond length was found to be 2.2427(18) Å, which is in accordance with *trans*-Ir^{III}(H)(OH₂) complexes described in literature.¹¹

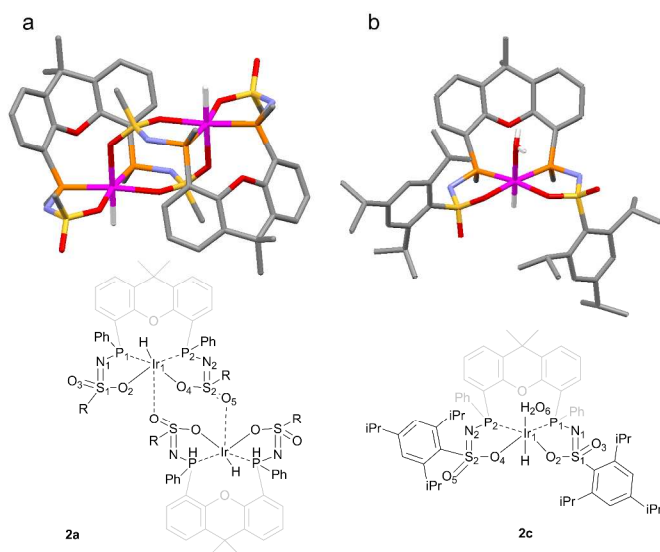


Fig 3. (a) Schematic representation and molecular structure of **2a**.^{4f} (b) Schematic representation and molecular structure of **2c**.¹⁴ Solvent molecules and H-atoms omitted for clarity, except for hydride and hydrogens of the aqua ligand. Color labels: purple: iridium, orange: phosphorus, blue: nitrogen, yellow: sulfur, red: oxygen. Selected bond lengths (Å) and angles (°) for **2c**: N₁-S₁ 1.554(2), N₂-S₂ 1.554(2), S₁-O₂ 1.4974(18), S₂-O₄ 1.5093(18), S₁-O₃ 1.4541(18), S₂-O₅ 1.439(2), Ir₁-P₁ 2.2311(6), Ir₁-P₂ 2.2315(6), Ir₁-O₂ 2.1639(18), Ir₁-O₄ 2.1752(17), Ir₁-O₆ (H₂O) 2.2427(18), P₁-Ir₁-P₂ 104.54(2).

Dehydrogenation studies with complexes **2a-c**

The catalytic dehydrogenation of HCOOH was investigated with complexes **2a-c**.[§] Catalysis was performed in toluene at 85 °C in the absence of base to generate dehydrogenation curves that are shown in Figure 4.[‡] The turnover frequencies (TOFs) of

3090 (**2a**), 877 (**2b**) and 1791 h⁻¹ (**2c**) reveal a correlation with the electronic nature of the sulfonamide organic side-group, i.e. high activity is obtained with an electron-donating group in *para*-position (**2a**, *n*-butyl), whereas an electron-withdrawing

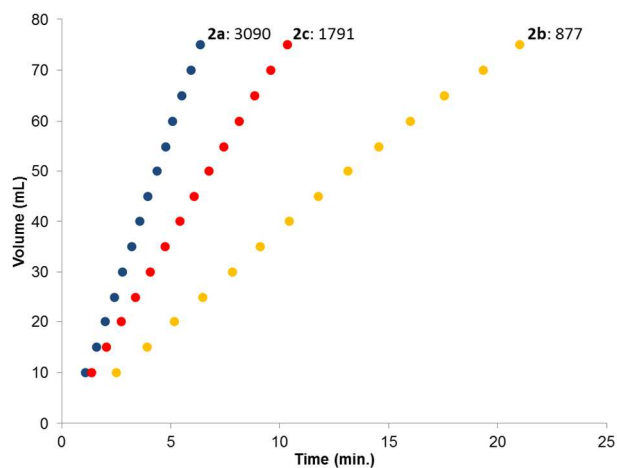


Fig 4. Dehydrogenation curves of **2a-c** (TOFs are determined between 4-30% conversion); total measured volume (mL) consist of both H₂ and CO₂.

group in *para*-position (**2b**, CF₃) results in much lower activity (see computational section for plausible explanation). Also with sterically encumbered complex **2c** a lower activity was obtained than with **2a**. Variable temperature (VT) NMR spectroscopy was performed to obtain mechanistic insight and detect relevant intermediates.[†] The addition of an equimolar amount of HCOOH to complex **2a** at 223 K led to a significant downfield shift (1.7 ppm) of one of the phosphorus signals (see Figure 5, left). This might indicate (partial) protonation of one of the ligand arms. Upon increasing the temperature to 298 K the original ³¹P NMR spectrum for species **2a** is instantaneously restored with no observation of any intermediates.[‡] Addition of one equivalent of HCOOH to **2a** results in an upfield shift at 223 K of the formate proton of 0.13 ppm (Figure 5 right) compared to free HCOOH, which is an indication of HCOOH coordination to the axial vacant site (Figure 5 top). Increasing the temperature leads to decreasing HCOOH signals together with the formation of H₂.

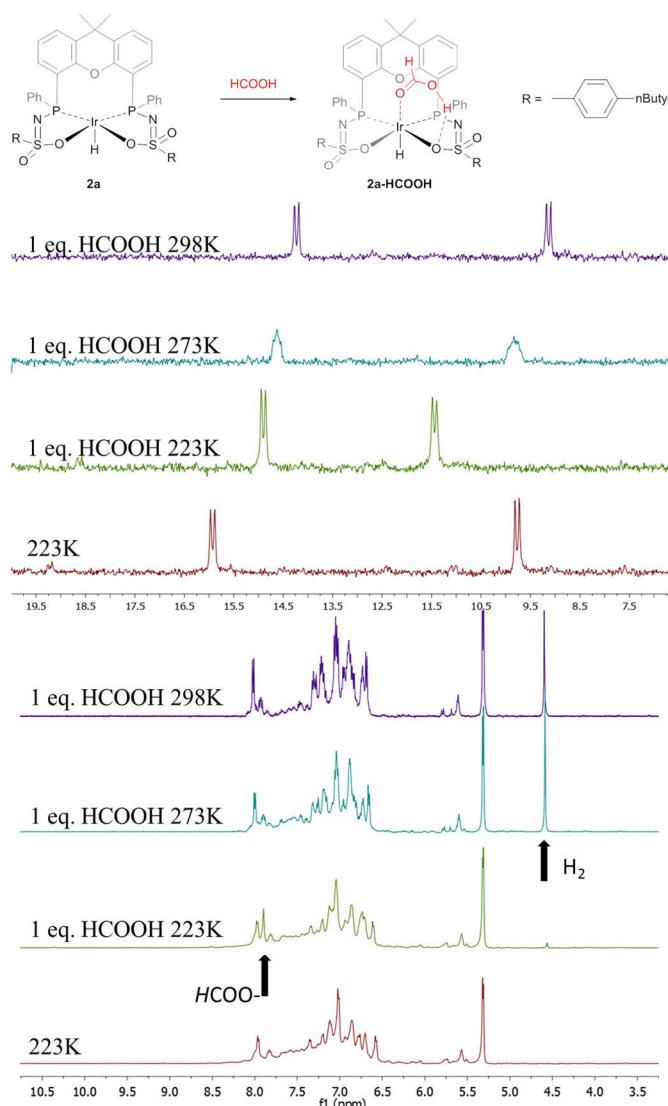


Fig 5. Proposed coordination of HCOOH to complexes **2** to form **2a-HCOOH** adduct (top). VT ^{31}P NMR spectra of **2a** with one equivalent of HCOOH (left). VT ^1H NMR spectra of **2a** with one equivalent of HCOOH; arrows indicate HCOO $^-$ -proton and H $_2$ formed (right).

Computational investigation into β -hydride elimination

The C-H bond cleavage in the dehydrogenation of HCOOH, typically the rate determining step in the catalytic cycle, can either occur via β -hydride elimination or via (ligand-assisted) direct hydride-transfer of the formate hydrogen (HCOOH) atom (see Figure 2A, B and C). Both possible mechanisms were computationally investigated using DFT in order to shed light on the potential role of the proton-responsive bisMETAMORPhos ligand. The obtained energy profiles for β -hydride elimination toward an equatorial and an axial coordination site of the catalyst are shown in Figure 6 (only the relevant part of the computed structures is shown).[¶]

The first step in the energy profile towards equatorial β -hydride elimination (red profile) is complete proton-transfer of HCOOH to the cooperative ligand, resulting in the formation of κ^1 -formate complex **3I**, which is endergonic by 11.3 kcal mol $^{-1}$. In

this structure the formate C-H bond is pre-organized for β -hydride elimination via high barrier transition state **3II** ($\Delta G^\ddagger = 32.2$ kcal mol $^{-1}$).[¶] This produces *cis*-dihydride structure **3III**, which is an overall exergonic process (-5.7 kcal mol $^{-1}$). Structure **3III** can release H $_2$ via protonation of an iridium hydride by the ligand (N-H or O-H) or reductive elimination of the two hydride units. Protonation of the hydride by the N-H moiety of the ligand in transition state **3IV** has a rather high barrier (red profile, 21.4 kcal mol $^{-1}$). No transition state was found for protonation of the hydride via an O-H group. Transition state **3IV** is potentially stabilized by axial coordination of the ligand via the sulfon group, which is in proximity to the iridium (2.42 Å). This stabilization cannot occur upon protonation via the O-H moiety, which potentially explains why no transition state could be found. The reductive elimination of H $_2$ forms Ir I structure **1** (similar to the initially formed complexes **1a-c** that lead to the formation of **2a-c**) via transition state **3IV'**, which is 4.6 kcal mol $^{-1}$ lower in energy (blue energy profile, 11.1 kcal mol $^{-1}$) than **3IV**. After release of H $_2$ the formed structure **1** is 6.4 kcal mol $^{-1}$ higher in energy than starting structure **2**. This is in agreement with experimental observations, as iridium(I) complexes **1a-c** eventually transform to the thermodynamically more stable iridium(III)-hydride complexes **2a-c**. The above described pathway to *cis*-dihydride species **3III** via transition state **3II** (Figure 6, red line) seems unlikely to occur, as the activation barrier obtained for C-H cleavage is rather high (32.2 kcal mol $^{-1}$). The β -hydride elimination towards the axial position was found to be energetically more favorable (Figure 6, black energy profile). Deprotonation of HCOOH by the ligand and formation of κ^1 -formate structure **4I** is endergonic by 4.1 kcal mol $^{-1}$. The protonated ligand showed a N-H \cdots O hydrogen bonding interaction between the ligand and the coordinated formate. β -Hydride elimination from **4I** via transition state **4II** to yield **4III** has an activation barrier of 26.3 kcal mol $^{-1}$. The *trans*-dihydride structure **4III** is slightly endergonic by 0.1 kcal mol $^{-1}$. Protonation of the Ir-H bond by a ligand N-H group to release H $_2$ from **4III** via transition state **4IV** has a high barrier of 24.0 kcal mol $^{-1}$. This is most likely related to the significant structural reorganization needed to bring the N-H proton in proximity to the hydride. Under catalytic conditions an excess of HCOOH is present, so we decided to investigate whether an additional equivalent of HCOOH could mediate the proton-transfer from the ligand to the Ir-H. Indeed, a transition state was obtained wherein protonation of the Ir-H with HCOOH occurred simultaneously with reprotonation of HCOOH by the ligand N-H (Figure 6, green profile). This transition state (**4IV'**) turned out to be 13.7 kcal mol $^{-1}$ lower in energy (10.3 kcal mol $^{-1}$) compared to transition state **4IV**. Similar second-sphere interactions were previously proposed in the heterolysis of H $_2$ assisted by exogenous water.¹² In our case, HCOOH provides a perfect geometrical fit between Ir-H and the N-H moiety of the ligand for second-sphere assisted proton transfer to occur.

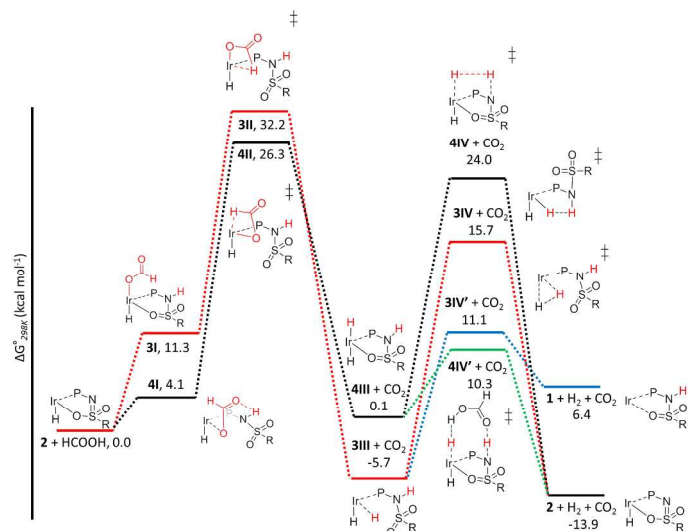


Fig 6. Potential energy diagram (DFT, BP86, def2-TZVP) for the dehydrogenation of formic acid via β -hydride elimination at the equatorial (red) and axial (black) position $\Delta G^{\ddagger}_{298K}$ is in kcal mol⁻¹.

Computational investigation into direct hydride-transfer

An alternative mechanism for the dehydrogenation of formic acid could involve a direct hydride-transfer of the formate hydrogen (HCOOH) to the Ir-center, subsequent to, or in concert with proton transfer of the acidic HCOOH proton to the ligand scaffold. In this mechanism a single metal coordination site is sufficient for effective turnover. To test the validity of such a pathway, we computed different HCOOH-2 adducts. Adducts with either axial or equatorial coordination were all found to exhibit stabilizing hydrogen-bonding interactions with either the nitrogen atom or the coordinated oxygen atom in the ligand scaffold, resulting in structures **5I-8I** (see Figure 7). Axial coordination of $\text{HCOOH} (**5I**; interaction with O) is the only structure found to be exergonic by 3.07 kcal mol⁻¹, compared to the free complex plus HCOOH . Formation of structure **6I**, with an N-H interaction, is endergonic by 3.82 kcal mol⁻¹. Equatorial coordination of HCOOH , leading to structure **7I** or **8I**, is associated with a significant energy-penalty of 11.8 (**7I**) or 13.8 (**8I**) kcal mol⁻¹ compared to formation of the axial adducts.$

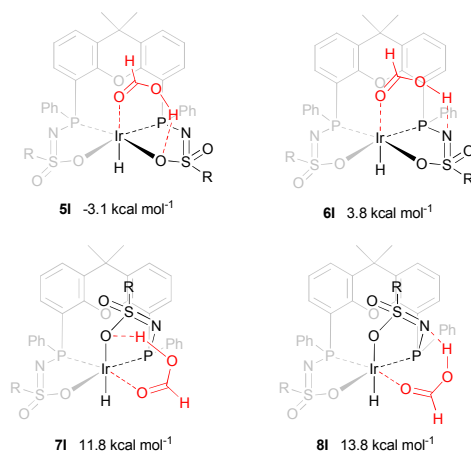


Fig 7. DFT optimized geometries of formic acid adducts **5I-8I** (BP86, def2-TZVP, ΔG°_{298K} in kcal mol⁻¹), R = phenyl.

The dehydrogenation of HCOOH via a direct hydride-transfer pathway was first investigated using the axial HCOOH adducts **5I** and **6I**. Starting from the energetically most stable structure **5I** (see black energy profile in Figure 8), an endergonic rearrangement to **5II** was found (+11.8 kcal mol⁻¹), which orients the formate hydrogen in a favorable position for direct hydride-transfer to the metal. In transition state **5III** ($\Delta G^{\ddagger} = 26.8$ kcal mol⁻¹ and $\Delta G^{\ddagger} = 29.9$ kcal mol⁻¹ with respect to **5I**) HCOOH is fully deprotonated by the ligand. This enables facile expulsion of CO_2 leading to a 6-membered $\text{Ir}\cdots\text{H}\cdots\text{C}\cdots\text{O}\cdots\text{H}\cdots\text{O}$ transition state. After release of CO_2 , dihydride complex **5IV** is formed in an overall endergonic process (+16.9 kcal mol⁻¹), whereafter protonation of the iridium-hydride via transition state **5V** (+17.4 kcal mol⁻¹) releases H_2 . The HCOOH dehydrogenation pathway was also investigated starting from structure **6I** (red profile in Figure 8). The rearrangement from **6I** to **6II** (similar to the rotation of **5I** to **5II**) is endergonic by 12.8 kcal mol⁻¹. However, transition state **6III** was found to be significantly lower in energy ($\Delta G^{\ddagger} = 20.2$ kcal mol⁻¹) compared to **5III** ($\Delta G^{\ddagger} = 26.8$ kcal mol⁻¹), leading to formation of structure **4III** via an unusual 8-membered $\text{Ir}\cdots\text{H}\cdots\text{C}\cdots\text{O}\cdots\text{H}\cdots\text{N}\cdots\text{S}\cdots\text{O}$ transition state, see Figure 6. Structures **6I-III** are all stabilized by hydrogen bonding interactions between HCOOH/CO_2 and the ligand pre-assembling HCOOH and stabilizing the transition state. The same role of the ligand was found in the energy profile starting from structure **5I**. The Ir-H and N-H bonds in transition state **6III** are elongated compared to those found in **4III** (Ir-H: 1.76 Å vs. 1.67 Å; N-H: 1.04 Å vs. 1.02 Å), which indicates a late transition state (Figure 9). A similar interaction was proposed by Hazari *et al.* for CO_2 insertion of an Ir-H stabilized by hydrogen bonding between a ligand-based N-H group and CO_2 .¹³ Calculations performed on structures lacking these H-bonding interactions (by pointing the N-H fragment outwards) yielded unstable structures and no transition states could be found. After CO_2 release from **6III**, structure **4III** is formed that releases H_2 with assistance of another molecule of HCOOH

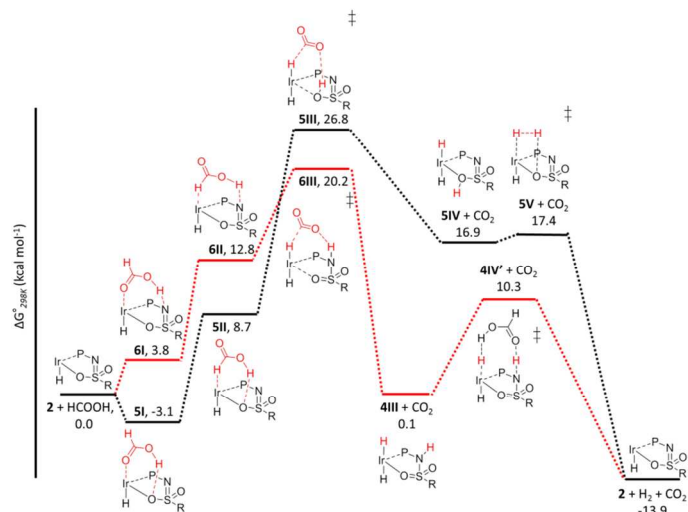


Fig 8. Potential energy diagram (DFT, BP86, def2-TZVP) for dehydrogenation of formic acid by **5I** (black profile) and **6I** (red profile); $\Delta G^{\ddagger}_{298K}$ is in kcal mol⁻¹.

(structure **4IV'**), regenerating the catalyst as described above (Figure 6, green profile). Direct hydride-transfer was also investigated starting from structures **7I** and **8I**, but these energy profiles were found to be significantly higher than for **5I** and **6I**.[‡]

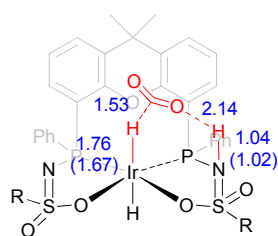
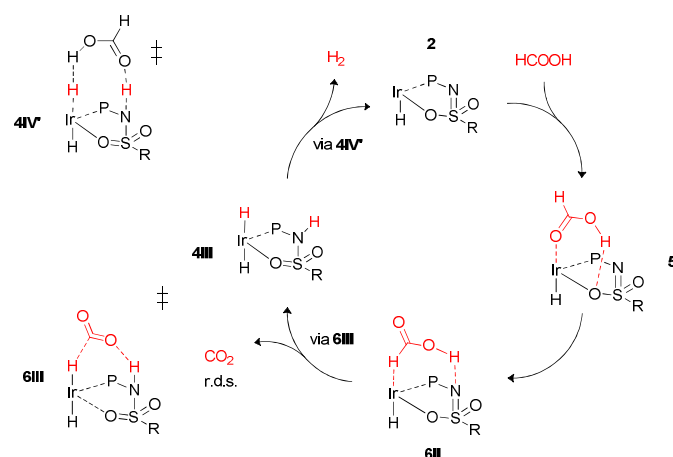


Fig 9. Transition state **6III** with stabilizing hydrogen-bond between ligand and CO₂. Relevant computed bond lengths (in Å) are compared to values found computationally for structure **4III** (in parentheses).

These calculations suggest that HCOOH dehydrogenation using bisMETAMORPhos-derived complexes **2a-c** follows an outer-sphere direct hydride-transfer mechanism at the axial vacant site of these monohydride species. Starting from formic acid adduct **5I**, the energetically most favored pathway requires rearrangement of **5I** to **6I**. This is likely a facile process due to the high proton-mobility within the ligand scaffold (from N-H to O-H), as was also inferred from the rapid proton-shuttling in complexes **1a-c**. This results in an overall activation barrier of 23.3 kcal mol⁻¹, taking **5I** as the resting state. This is in agreement with the variable temperature ¹H NMR observations, as the change in chemical shift upon addition of HCOOH to **2a** indicates the formation of a **2a**-HCOOH adduct akin to structure **5I**. Protonation of the ligand takes place in transition state structure **6III**. The hydride ligand already present in complexes **2a-c**, *trans* to the axial coordination site of HCOOH, acts purely as a spectator ligand. The lower activity of complex **2c**, bearing electron-withdrawing CF₃ groups, can therefore

potentially be explained by the decreased basicity of the nitrogen atom in the ligand. The electronic effect was also investigated theoretically by comparing *p*-CF₃ with *p*-CH₃ substituents. Indeed, a higher activation barrier was found for *p*-CF₃ (24 kcal mol⁻¹) compared to *p*-CH₃ (22.5 kcal mol⁻¹), see ESI for energy profiles. We propose the following overall dual-role for the bisMETAMORPhos ligand in the mechanism of formic acid dehydrogenation (Scheme 3). Species **2** coordinates HCOOH at the vacant axial site, aided by hydrogen-bonding with the coordinated sulfon-oxygen atom to give structure **5I**. Reorientation of the formate group gives a pre-activated HCOOH unit that has hydrogen-bonding with the deprotonated nitrogen of the ligand arm (**6II**). Release of CO₂ is achieved via transition state **6III** (rate determining step) wherein the ligand deprotonates HCOOH and stabilizes the direct hydride transfer by a hydrogen bonding interaction. This gives *trans*-dihydride **4III** that releases H₂ aided by an additional equivalent of HCOOH, which protonates the Ir-H and in turn is reprotonated by the ligand, thereby regenerating starting complex **2**. The reversibility of this catalytic system is currently under investigation.



Scheme 3. Schematic proposed catalytic cycle of the ligand assisted dehydrogenation of HCOOH by bisMETAMORPhos complexes **2a-c**.

Conclusions

We report several bisMETAMORPhos ligands (**La-Lc**) based on the xanthene backbone bearing two sulfonamidophosphine units. The prototropic nature of these PN(H)SO₂R fragments results in different ratios for the P^{III} and P^V tautomers, depending on the electronic and steric nature of the sulfonamide substituents. Formation of Ir^I complexes **1a-c** was achieved by coordination of **La-Lc** to Ir(acac)(cod). Subsequent formal oxidative addition of the remaining N-H group resulted in the formation of the corresponding Ir^{III}-monohydride complexes Ir^{III}(H)(L) (**2a-c**). These three complexes are active catalysts for the base-free dehydrogenation of formic acid, with TOFs of 3090, 877 and 1791 h⁻¹ for **2a-c**, respectively. These data reflect the influence of subtle electronic and steric changes in the ligand architecture. The role of the ligand during

catalysis was investigated by variable temperature ^1H and ^{31}P NMR spectroscopic measurements and DFT calculations. Variable temperature NMR data point to the formation of a **2a**-HCOOH adduct. DFT calculations indicate that the hydrogen-bonding abilities of the ligand play an important role in the mechanism, resulting in an uncommon direct hydride-transfer mechanism instead of the more commonly proposed β -hydride elimination for HCOOH dehydrogenation. This was also found to be the rate-determining step ($23.3 \text{ kcal mol}^{-1}$), which confirms experimental observations using DCOOH and HCOOD.^{4f} A similar mechanism has been proposed for Al- and Fe-based systems reported by Berben and Milstein, respectively.^{6c, 8c} It was found that the combined hydrogen-bonding and proton-responsive properties of the bisMETAMORPhos ligands are essential for the reactivity of complexes **2a-c**. These interactions facilitate the pre-assembly of the HCOOH substrate and the stabilization of catalytically relevant intermediates and transition states, allowing an otherwise inaccessible reaction pathway. We thus show that a single coordination site is effective for the dehydrogenation reaction to occur when using a functional ligand scaffold. The proton-responsive and hydrogen-bonding features of ligands (**La-Lc**) are currently being explored for other reactions. The mechanistic findings presented herein potentially play a role with other HCOOH dehydrogenative catalysts bearing hydrogen-bonding functionalities in their ligand systems.

Acknowledgements

We kindly acknowledge NWO for financial support, Frédéric G. Terrade and Dániel L. J. Broere for fruitful discussions and Ed Zuidinga for mass analysis.

Notes and references

^a S. Oldenhof, Prof. Dr. B. de Bruin, Dr. Ir. J. I. van der Vlugt, Prof. Dr. J. N. H. Reek, van 't Hoff Institute for Molecular Sciences, University of Amsterdam, Science Park 904, 1098 XH, Amsterdam (The Netherlands), E-mail: j.n.h.reek@uva.nl

^b Dr. M. Lutz, Bijvoet Center for Biomolecular Research Utrecht University, Padualaan 8, 3584 CH Utrecht (The Netherlands).

‡ See supporting information.

§ Dehydrogenation studies were performed with the diastereomeric mixtures of complexes **2a-c** (upon anionic coordination of the sulfon group these become chiral and give rise to diastereomeric mixtures of the complexes **2**) see supporting information and reference 4f for more information.

† VT-NMR studies were performed with diastereomerically pure form of **2a** see reference 4f for additional information.

δ The ^{31}P NMR chemical shifts of **2a** are significantly affected by the temperature, but these changes are completely reversible, see supporting information.

¶ Note that these are gas-phase calculations for which the translational entropy contributions are much larger than in solution. By calculation of the partition function of the molecules in the gas phase, the entropy of dissociation or coordination for reactions in solution is overestimated

Therefore, for reactions in solution, the Gibbs free energies for all steps involving a change in the number of species should be corrected. Several methods have been proposed for corrections of gas phase to solution phase data. The minimal correction term is a correction for the condensed phase (CP) reference volume (1 L mol^{-1}) compared to the gas phase (GP) reference volume (24.5 L mol^{-1}). This leads to an entropy correction term ($\text{SCP} = \text{SGP} + R\ln\{1/24.5\}$) for all species, lowering the relative free energies (298 K) of all associative steps with $2.5 \text{ kcal mol}^{-1}$.¹⁵ According to some authors, this correction term is too small, and larger correction terms up to $6.0 \text{ kcal mol}^{-1}$ have been suggested.¹⁶ Which correction term is best remains a bit debatable.

ψ All calculations were performed with R = phenyl on the sulfon group for computational simplicity using the diastereomeric form that was utilized in VT NMR studies and obtained as crystal structure.

Electronic Supplementary Information (ESI) available: [details of any supplementary information available should be included here]. See DOI: 10.1039/b000000x/

- (a) M. Raynal, P. Ballester, A. Vidal-Ferran, P. W. N. M. van Leeuwen, *Chem. Soc. Rev.* 2014, **43**, 1734-1787; (b) M. Raynal, P. Ballester, A. Vidal-Ferran, P. W. N. M. van Leeuwen, *Chem. Soc. Rev.* 2014, **43**, 1660-1733; (c) T. S. Koblenz, J. Wassenaar, J. N. H. Reek, *Chem. Soc. Rev.* 2008, **37**, 247-262.
- (a) B. Breit, W. Seiche, *J. Am. Chem. Soc.* 2003, **125**, 6608-6609; (b) S. Zhu, J. V. Ruppel, H. Lu, L. Wojtas, X. P. Zhang, *J. Am. Chem. Soc.* 2008, **130**, 5042-5043. (c) J. Meeuwissen, M. Kuil, A. M. van der Burg, A. J. Sandee, J. N. H. Reek, *Chemistry – A European Journal* 2009, **15**, 10272-10279; (d) L. Diab, T. Šmejkal, J. Geier, B. Breit, *Angew. Chem. Int. Ed.* 2009, **48**, 8022-8026; for reviews see: (e) J. Meeuwissen, J. N. H. Reek, *Nat. Chem.* 2010, **2**, 615-621; (f) A. J. Sandee, J. N. H. Reek, *Dalton Trans.* 2006, 3385-3391; (g) S. Carboni, C. Gennari, L. Pignataro, U. Piarulli, *Dalton Trans.* 2011, **40**, 4355-4373.
- (a) S. Das, C. D. Incarvito, R. H. Crabtree, G. W. Brudvig, *Science* 2006, **312**, 1941-1943; (b) L. Du, P. Cao, J. Xing, Y. Lou, L. Jiang, L. Li, J. Liao, *Angew. Chem. Int. Ed.* 2013, **52**, 4207-4211; (c) P. Dydio, J. N. H. Reek, *Chem. Sci.* 2014, **5**, 2135-2145; (d) D. B. Grotjahn, *Chem. Eur. J.* 2005, **11**, 7146-7153; (e) T. Šmejkal, B. Breit, *Angew. Chem. Int. Ed.* 2008, **47**, 311-315; (f) P.-A. R. Breuil, F. W. Patureau, J. N. H. Reek, *Angew. Chem. Int. Ed.* 2009, **48**, 2162-2165; (g) P. Dydio, W. I. Dzik, M. Lutz, B. de Bruin, J. N. H. Reek, *Angew. Chem. Int. Ed.* 2011, **123**, 416-420; (h) P. Dydio, C. Rubay, T. Gadzikwa, M. Lutz, J. N. H. Reek, *J. Am. Chem. Soc.* 2011, **133**, 17176-17179; (i) P. Dydio, J. N. H. Reek, *Angew. Chem. Int. Ed.* 2013, **52**, 3878-3882; (j) Y. Gumrukcu, B. de Bruin, J. N. H. Reek, *ChemSusChem* 2014, **7**, 890-896. (k) H. Lu, W. I. Dzik, X. Xu, L. Wojtas, B. de Bruin, X. P. Zhang, *J. Am. Chem. Soc.* 2011, **133**, 8518-8521 (l) V. Lyaskovskyy, A. I. O. Suarez, H. Lu, H. Jiang, X. P. Zhang, B. de Bruin, *J. Am. Chem. Soc.* 2011, **133**, 12264-12273, (m) A. I. O. Suarez, H. Jiang, X. P. Zhang, B. de Bruin, *Dalton Trans.* 2011, **40**, 5697-5705; (n) for a recent review see: P. Dydio, J. N. H. Reek, *Chem. Sci.* 2014, **5**, 2135-2145.
- (a) F. W. Patureau, M. Kuil, A. J. Sandee, J. N. H. Reek, *Angew. Chem. Int. Ed.* 2008, **47**, 3180-3183; (b) F. W. Patureau, S. de Boer, M. Kuil, J. Meeuwissen, P.-A. R. Breuil, M. A. Siegler, A. L. Spek, A. J. Sandee, B. de Bruin, J. N. H. Reek, *J. Am. Chem. Soc.* 2009,

- 131, 6683-6685; (c) T. León, M. Parera, A. Roglans, A. Riera, X. Verdaguier, *Angew. Chem. Int. Ed.* 2012, **51**, 6951-6955; (d) F. W. Patureau, M. A. Siegler, A. L. Spek, A. J. Sandee, S. Jugé, S. Aziz, A. Berkessel, J. N. H. Reek, *Eur. J. Inorg. Chem.* 2012, **3**, 496-503; (e) F. G. Terrade, M. Lutz, J. I. van der Vlugt, J. N. H. Reek, *Eur. J. Inorg. Chem.* 2014, **10**, 1826-1835; (f) S. Oldenhof, B. de Bruin, M. Lutz, M. A. Siegler, F. W. Patureau, J. I. van der Vlugt, J. N. H. Reek, *Chem. Eur. J.* 2013, **19**, 11507-11511.
- 5 (a) R. Hille, *Chem. Rev.* 1996, **96**, 2757-2816; (b) C. M. P. T. Reda, N. J. Abram, J. Hirst, *Proc. Natl. Acad. Sci. USA* 2008, **105**, 10654-10658; (c) M. J. Romao, *Dalton Trans.* 2009, 4053-4068; (d) C. Mota, M. Rivas, C. Brondino, I. Moura, J. G. Moura, P. González, N. F. S. A. Cerqueira, *J. Biol. Inorg. Chem.* 2011, **16**, 1255-1268; (e) M. Tiberti, E. Papaleo, N. Russo, L. De Gioia, G. Zampella, *Inorg. Chem.* 2012, **51**, 8331-8339; (f) K. Schuchmann, V. Müller, *Science* 2013, **342**, 1382-1385.
- 6 (a) A. Boddien, D. Mellmann, F. Gärtner, R. Jackstell, H. Junge, P. J. Dyson, G. Laurenczy, R. Ludwig, M. Beller, *Science* 2011, **333**, 1733-1736; (b) J. F. Hull, Y. Himeda, W.-H. Wang, B. Hashiguchi, R. Periana, D. J. Szalda, J. T. Muckerman, E. Fujita, *Nat. Chem.* 2012, **4**, 383-388; (c) T. Zell, B. Butschke, Y. Ben-David, D. Milstein, *Chem. Eur. J.* 2013, **19**, 8068-8072; (d) E. A. Bielinski, P. O. Lagaditis, Y. Zhang, B. Q. Mercado, C. Würtele, W. H. Bernskoetter, N. Hazari, S. Schneider, *J. Am. Chem. Soc.* 2014, **136**, 10234-10237; (e) Y. Manaka, W.-H. Wang, Y. Suna, H. Kambayashi, J. T. Muckerman, E. Fujita, Y. Himeda, *Catal. Sci. Technol.* 2014, **4**, 34-37; (f) W.-H. Wang, S. Xu, Y. Manaka, Y. Suna, H. Kambayashi, J. T. Muckerman, E. Fujita, Y. Himeda, *ChemSusChem* 2014, **7**, 1976-1983.
- 7 (a) S. Kuwata, T. Ikariya, *Chem. Eur. J.* 2011, **17**, 3542-3556; (b) S. Schneider, J. Meiners, B. Askevold, *Eur. J. Inorg. Chem.* 2012, **3**, 412-429; (c) J. I. van der Vlugt, *Eur. J. Inorg. Chem.* 2012, **3**, 363-375; (d) B. Zhao, Z. Han, K. Ding, *Angew. Chem. Int. Ed.* 2013, **52**, 4744-4788; (e) G. A. Filonenko, M. P. Conley, C. Copéret, M. Lutz, E. J. M. Hensen, E. A. Pidko, *ACS Catal.* 2013, **3**, 2522-2526; (f) D. V. Gutsulyak, W. E. Piers, J. Borau-García, M. Parvez, *J. Am. Chem. Soc.* 2013, **135**, 11776-11779; (g) C. M. Moore, N. K. Szymczak, *Chem. Commun.* 2013, **49**, 400-402; (h) G. Zhang, K. V. Vasudevan, B. L. Scott, S. K. Hanson, *J. Am. Chem. Soc.* 2013, **135**, 8668-8681.
- 8 (a) G. A. Filonenko, E. J. M. Hensen, E. A. Pidko, *Catal. Sci. Technol.* 2014, **4**(10), 3474-3485; (b) T. J. Schmeier, G. E. Dobreiner, R. H. Crabtree, N. Hazari, *J. Am. Chem. Soc.* 2011, **133**, 9274-9277; (c) T. W. Myers, L. A. Berben, *Chemical Science* 2014, **5**, 2771-2777.
- 9 (a) T. Koike, T. Ikariya, *Adv. Synth. Catal.* 2004, **346**, 37-41; (b) P. Š. J. Václavík, B. Vilhanová, J. Pecháček, M. Kuzma, P. Kačer, *Molecules* 2013, **18**, 6804-6828; (c) A. Nova, D. J. Taylor, A. J. Blacker, S. B. Duckett, R. N. Perutz, O. Eisenstein, *Organometallics* 2014, **33**, 3433-3442.
- 10 (a) R. Sánchez-de-Armas, L. Xue, M. S. G. Ahlquist, *Chem. Eur. J.* 2013, **19**, 11869-11873; (b) X. Yang, *Dalton Trans.* 2013, **42**, 11987-11991.
- 11 (a) H. Bauer, U. Nagel, W. Beck, *J. Organomet. Chem.* 1985, **290**, 219-229; (b) M. Feller, A. Karton, G. Leitus, J. M. L. Martin, D. Milstein, *J. Am. Chem. Soc.* 2006, **128**, 12400-12401; (c) J. J. Adams, A. Lau, N. Arulsamy, D. M. Roddick, *Organometallics* 2011, **30**, 689-696.
- 12 (a) C. Yin, Z. Xu, S.-Y. Yang, S. M. Ng, K. Y. Wong, Z. Lin, C. P. Lau, *Organometallics* 2001, **20**, 1216-1222; (b) M. S. G. Ahlquist, *J. Mol. Catal. A: Chem.* 2010, **324**, 3-8; (c) X. Yang, *ACS Catal.* 2011, **1**, 849-854; (d) R. Tanaka, M. Yamashita, L. W. Chung, K. Morokuma, K. Nozaki, *Organometallics* 2011, **30**, 6742-6750; (e) A. Pavlova, E. J. Meijer, *ChemPhysChem* 2012, **13**, 3492-3496.
- 13 T. J. Schmeier, G. E. Dobreiner, R. H. Crabtree, N. Hazari, *J. Am. Chem. Soc.* 2011, **133**, 9274-9277.
- 14 CCDC 1020151 contains the supplementary crystallographic data for this paper. These data can be obtained free of charge from The Cambridge Crystallographic Data Centre via www.ccdc.cam.ac.uk/data_request/cif.
- 15 (a) W. I. Dzik, X. Xu, P. Zhang, J. N. H. Reek, B. de Bruin, *J. Am. Chem. Soc.* **2010**, **132**, 10891-10902. (b) A. J. C. Walters, J. N. H. Reek, B. de Bruin, *ACS Catalysis*, **2014**, **4**, 1376-1389.
- 16 (a) D. H. Wertz, *J. Am. Chem. Soc.* **1980**, **102**, 5316-5322. (b) N. Schneider, M. Finger, C. Haferkemper, S. Bellemin-Laponnaz, P. Hofmann, L. Gade, *Angew. Chem., Int. Ed.* **2009**, **48**, 1609-1613